Conformational Changes in Human Serum Albumin Induced by Sodium Perfluorooctanoate in Aqueous Solutions

Paula V. Messina,† Gerardo Prieto,* Juan M. Ruso, and Félix Sarmiento

Grupo de Biofísica e Interfases, Departamento de Física Aplicada, Facultad de Física, Universidad de Santiago de Compostela, 15782 Santiago de Compostela, Spain

Received: March 5, 2005; In Final Form: May 30, 2005

Conformational changes in the bulk solution and at the air−aqueous interface of human serum albumin (HSA) induced by changes in concentration of sodium perfluorooctanoate ($C_7F_{15}COO^-Na^+$) were studied by difference spectroscopy, ζ-potential data, and axisymmetric drop shape analysis. ζ-potential was used to monitor the formation of the HSA−$C_7F_{15}COO^-Na^+$ complex and the surface charge of the complex. The conformational transition of HSA in the bulk solution was followed as a function of denaturant concentration by absorbance measurements at 280 nm. The data were analyzed to obtain values for the Gibbs energies of the transition in water (ΔG^0_W) and in a hydrophobic environment (ΔG^0_{hc}) pertaining to saturated protein−surfactant complexes. The conformational changes that surfactants induce in HSA molecules alter its absorption behavior at the air−water interface. Dynamic surface measurements were used to evaluate this behavior. At low [$C_7F_{15}COO^-Na^+$], proteins present three adsorption regimes: induction time, monolayer saturation, and interfacial gelation. When surfactant concentration increases and conformational changes in the bulk solution occur, the adsorption regimes disappear. HSA molecules in an intermediate conformational state migrate to the air−water interface and form a unique monolayer. At high [$C_7F_{15}COO^-Na^+$], the adsorption of denatured molecules exhibits a behavior analogous to that of dilute solutions.

Introduction

Human serum albumin (HSA) is the most abundant protein in plasma. It contains 585 amino acid residues and is 55% helical with no β strands. There are 17 disulfide bonds within three domains. Two of the domains contain binding sites for fatty acids and one is nonbinding. The single polypeptide contains internal hydrophobic "pockets" which house the hydrocarbon tails of the fatty acids and several differently charged residues electrostatically binding the carboxylic ends. Albumin function for all transport stages is based on high conformation flexibility of the protein molecule and on the liability of its binding-site characteristics. Comparison of the structure of liganded and unliganded HSA reveals dramatic conformational changes upon fatty acid binding.[1] As the major soluble protein constituent of the circulatory system, HSA has many physiological and pharmacological functions. It contributes to colloid osmotic blood pressure[2] and is chiefly responsible for the maintenance of blood pH.[3] Moreover, it also plays an important role in the transport and disposition of endogenous and exogenous ligands present in blood.[2] Its surprising capacity to bind a large variety of drugs results in its prevailing role in drug pharmacokinetics and pharmacodynamics. Its primary pharmacokinetics function is participating in adsorption, distribution, metabolism, and excretion of drugs. However, drug distribution is controlled by HSA to a greater extent, because most drugs travel in plasma and reach the target tissues by binding to HSA.[4] Strong binding can decrease the concentration of free drug in plasma, whereas weak binding can lead to a short lifetime or poor distribution. Hence, it is important to study the interactions between a new compound having biological activity and HSA.

Fluorinated surfactants can be used to generate and stabilize various colloidal systems, including different types of emulsions, vesicles, and tubules. This feature also seems promising for controlled-release drug delivery.

Various researchers have studied the structure and properties of serum albumin and its interactions with other proteins and with surfactants to understand serum albumin functionality, which have been included in novel applications. The effects of binding and conformational changes induced by anionic sodium dodecyl sulfate (SDS) and sodium octyl sulfate (SOS), cationic cethyltrimethylammonium chloride (CTAC), and zwitterionic *N*-hexadecyl-*N*,*N*-dimethyl-3-ammonium-1-propanesulfonate (HPS) surfactants on bovine serum albumin (BSA) and HSA have been studied using differential scanning calorimetry (DSC), circular dichroism (CD), fluorescence, and UV spectroscopic methods.[5,6]

Until recently, few fluorinated surfactants had been reported enough to be utilized in pharmaceuticals. The biological effects, pharmacology, toxicity, and protein interactions with such surfactants have been investigated.[7−9]

In previous works, we evaluated the binding of two different surfactants, hydrogenated (sodium octanoate) and fluorinated (sodium perfluorooctanoate), to three proteins (lysozyme, hemoglobin, and catalase) by the measurement of ζ-potential[10] and studied the interplay between HSA and sodium perfluorooctanoate ($C_7F_{15}COO^-Na^+$) in dilute solutions using a recently developed method, axisymmetric drop shape analysis (ADSA), which is based on dynamic surface tension measurements.[11] Our results suggested that in dilute solutions protein molecules, as well as $C_7F_{15}COO^-Na^+$ molecules, tend to go to the aqueous−air interface. Under these conditions, protein and surfactant

* Corresponding author. Tel.: +34 981 563 100. Fax: +34 981 520 676. E-mail address: faxera@usc.es.

† Permanent address: Grupo de Ciencia de Superficies y Coloides, Departamento de Química, Universidad Nacional del Sur, 8000 Bahía Blanca, Argentina.

10.1021/jp051655v CCC: $30.25
Published on Web 07/22/2005

molecules in the bulk solution are negligible and interactions occur only at the interface. $C_7F_{15}COO^-Na^+$ induced conformational changes in HSA molecules at the air−aqueous interface.

In this work, the binding of sodium perfluorooctanoate to HSA was investigated at concentrated solutions by dynamic tension measurements combined with other methods, such as UV−vis spectrophotometric techniques and electrophoretic mobility measurements. The study revealed that $C_7F_{15}COO^-Na^+$ induces conformational changes in HSA molecules in the bulk solution, affecting protein adsorption at the air−aqueous interface.

Experimental Section

Materials. Sodium perfluorooctanoate, $C_7F_{15}COO^-Na^+$ (analytical grade (97%), product no. 16988), was from Lancaster MTM Research Chemicals Ltd. Human serum albumin (HSA, albumin ≥96%, essentially fatty acid free, product no. A-1887) was purchased from Sigma Chemical Co. It has a molecular weight of 66 500 Da and contains 585 amino acid residues. All chemicals were used without further treatment.

Preparation of Solutions. Sodium perfluorooctanoate ($C_7F_{15}COO^-Na^+$) and HSA stock solutions (1 mg/mL) were prepared by directly dissolving the appropriate amount of surfactant and protein in ultrapure water. Both solutions were kept in a refrigerator and diluted as required.

HSA solutions were prepared without buffer addition given how its presence could affect surface tension measurements. For a 5−8 pH range, no changes were observed in the three structural domains (I, II, and III) of HSA.[12] All experiments were performed at 25 ± 0.01 °C.

Apparatus and Methods. Surface tension measurements were made using mixed solutions containing 0.015 mM HSA and $C_7F_{15}COO^-Na^+$ at a 0.16−0.57 mM concentration range.

The experiments were performed with a constant pressure penetration Langmuir balance based on ADSA.

The whole setup, including image capturing, the microinjector, the ADSA algorithm, and the fuzzy pressure control, was managed by a Windows integrated program (DINATEM). A solution droplet is formed at the tip of the coaxial double capillary, connected to a double microinjector.

The program fits experimental drop profiles, extracted from digital drop micrographs, to the Young−Laplace equation of capillarity by using ADSA, and provides as output the drop volume V, the interfacial tension γ, and the surface area A. Pressure and area control use a modulated fuzzy logic PID algorithm (proportional, integral and derivative control). They are controlled by changing the drop volume. The isotherms are generated by changing the drop volume in a controlled manner and simultaneously measuring surface tension and keeping surface area constant (34 nm^2).

The sample solution formed a pendant drop at the tip of a capillary, enclosed in a quartz cuvette, which was mounted in an environmental chamber during the experiment. In each run, drop images were captured at 2, 10, and 60 s intervals for a period of 298, 7200, and 7440 s, respectively. Each experiment was repeated at least twice.

Difference spectra were measured with a Beckman spectrophotometer (model DU 640), with six microcuvettes, which operates in UV−vis region, from 190 to 1100 nm, of the electromagnetic spectrum wavelength. All measurements were made using HSA−$C_7F_{15}COO^-Na^+$ mixed solutions and 0.0188 mM HSA solutions containing $C_7F_{15}COO^-Na^+$ at a (0.1−30 mM) concentration range, in a pair of carefully matched quartz cuvettes (1 cm^3 capacity) in the wavelength range of 240−310 nm. Measurements were taken after HSA and the surfactant had been incubated for 24 h.

At least five measurements of difference spectra and surface tension were made.

ζ-potentials of the HSA system were measured using a Malvern Instruments Zetamaster 5002 by averaging 10 measurements at stationary level. The cell used was a 5 mm × 2 mm rectangular quartz capillary. The temperature of the experiments was 25 ± 0.01 °C and controlled by a Haake temperature controller. The ζ-potentials were calculated from the electrophoretic mobility, μ_E, by means of the Henry correction of Smoluchowski's[13] equation

$$\zeta = \frac{3\mu_E\eta}{2\epsilon_0\epsilon_r}\frac{1}{f(\kappa a)}$$

where ϵ_0 is the permittivity of the vacuum, ϵ_r is the relative permittivity, a is the particle radius, κ is the Debye length, and η is the viscosity of water. The function $f(\kappa a)$ depends on the particle shape and for our system was determined by

$$f(\kappa a) = \frac{3}{2} - \frac{9}{2\kappa a} + \frac{75}{2\kappa^2 a^2}$$

which is valid for $\kappa a > 1$.

Apart from some fundamental constants, κ depends only on the temperature and the bulk electrolyte concentration

$$\kappa = \left(\frac{2000F^2}{\epsilon_0\epsilon_r RT}\right)^{1/2}\sqrt{I}$$

where F is Faraday's constant and I is the ionic strength ($I = 1/2\Sigma c_i z_i^2$ where c_i is the ionic concentration in mol L^{-1} and z_i is the charge of the ion).

For our system, the radius of HSA molecules, a, was 4.5 nm[1] and κ calculated in the surfactant concentration range varied from 1.04 to 18.01 nm^{-1}, so the calculated κa values (from 4.68 to 81.04) were always >1.

To compare the results obtained, the same $C_7F_{15}COO^-Na^+$/HSA ratio range, 5.319−1595 mmol of $C_7F_{15}COO^-Na^+$/ mmol of HSA, was used for this study.

Results and Discussion

Conformational Changes in the Bulk Solution. The albumin molecule undergoes several well-organized changes in conformation, usually under nonphysiological conditions[14] (Figure 1). The N−F transition involves the unfolding of domain III.[15,16] The F form is characterized by a dramatic increase in viscosity, much lower solubility, and a significant loss in helical content.[17] At pH values lower than 4, albumin undergoes another expansion with the loss of the intradomain helices of domain I, which is connected to the helix of domain II, and the helix of domain II connected to the helix of domain III. This expanded form is known as the E form, which has an increased intrinsic viscosity and a rise in the hydrodynamic axial ratio from about 4 to 9. At pH 9, albumin changes conformation to the basic form B. If solutions of albumin are maintained at pH 9 and low ionic strength at 3 °C for 3−4 days, another isomerization occurs, known as the A form.[18] We studied the conformational changes in HSA molecules induced by the addition of $C_7F_{15}COO^-Na^+$ in aqueous solutions.

Figure 2 shows a plot of the ζ-potential of the protein−surfactant complex as a function of surfactant concentration at

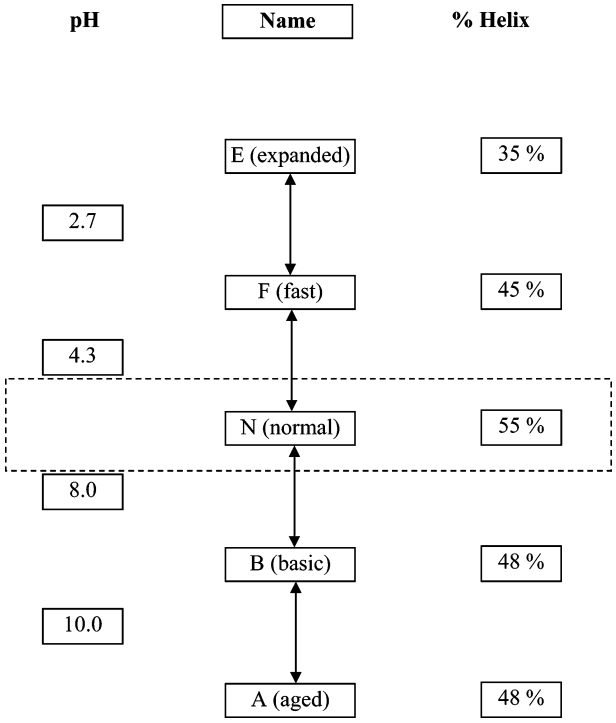

Figure 1. Interrelation of five recognized conformational forms of human serum albumin.

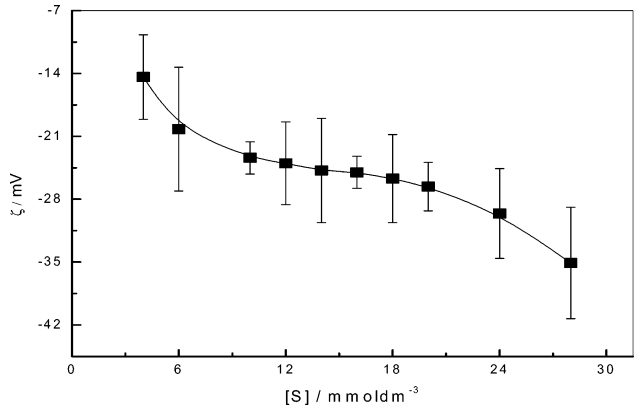

Figure 2. ζ−potential of the HSA−sodium perfluorooctanoate system at 25 °C.

25 °C. The addition of surfactant ($C_7F_{15}COO^-Na^+$) produces an increase in the effective net charge on the protein, suggesting the formation of the HSA−$C_7F_{15}COO^-Na^+$ complex. The adsorption of surfactant onto protein does not change the original ζ-potential sign, and all the negative values become more negative as the surfactant concentration increases. These negative values of ζ-potential suggest that the hydrophobic interaction is predominant.

The plots in Figure 3 show the absorbance changes for the 280 nm difference spectral band of HSA as a function of $C_7F_{15}COO^-Na^+$ concentration. There are two transition regions over which absorbance changes steeply with surfactant concentration. The first is a smooth change between the 9 and 13 mM surfactant, and the second is an abrupt change in a narrow range of surfactant concentration, between 15 and 17 mM, approximately. These results suggest that in the interaction with $C_7F_{15}COO^-Na^+$, HSA undergoes a significant change in conformation.

The absorption band at 280 nm is characteristic of tryptophan residues. Changes in protein conformation, such as unfolding, very often lead to large changes in the UV−vis emission. The

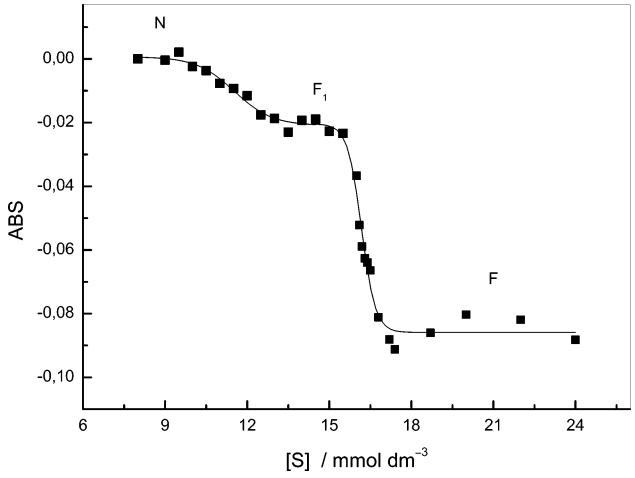

Figure 3. Absorbance variation of HSA at 280 nm vs [$C_7F_{15}COO^-Na^+$]. The HSA concentration was 0.0188 mM. Estimated uncertainties are less than 2%.

tryptophan emission of a native protein can be greater or smaller than the emission of free tryptophan in aqueous solution. Consequently, both increase and decrease in UV intensity can occur upon protein unfolding.

Initial addition of $C_7F_{15}COO^-Na^+$ (0.1−10 mM) does not have a significant effect on the tryptophan band intensity, but addition of (10−15 mM) surfactant results in a small decrease in the tryptophan emission. Additional surfactant (15−17 mM), around 16.3 mM, produces a strong decrease in the tryptophan emission due to protein unfolding. These findings seem to suggest that the conformational changes in protein molecules elapse in two steps.

The results are consistent with the literature. Foster's former student, Sogami, and others have found that the F isomerization, Figure 1, proceeds in two steps. The change in helicity observed at 233 nm and effects on fluorescence of both the HSA tryptophan[19] and a single bound ANS[20] lead to the proposal that the conformational change occurs first to an intermediate F_1 form, which then expands to the F form spontaneously, $N \rightarrow F_1 \rightarrow F$. The whole isomerization measured by stopped-flow analysis requires only about 100 ms.[21] It is fully reversible even from solutions of 8 M urea[22] within about 1 s.[23]

For the first approximation, the interaction between native HSA (N, normal state indicated in Figure 1) and surfactant (S) may be expressed by the equilibrium

$$N + \nu S \leftrightarrow DS_\nu \tag{1}$$

where ν is the average number of surfactant molecules bound to the complex (DS_ν). In writing eq 1, it is assumed that the binding of the surfactant and the conformational changes induced by binding are reversible. The reversibility of the difference spectral absorbance at 280 nm in surfactant dilutions from high to lower concentrations suggests that this is a reasonable assumption. The equilibrium constant (K) for reaction 1 can thus be written as

$$K = \frac{[DS_\nu]}{[N][S]^\nu} = \frac{K_S}{[S]^\nu} \tag{2}$$

where K_S is the ratio of surfactant−protein complex and native molecules, and [S] is the equilibrium concentration of free surfactant. Because HSA molarity was very low (0.0188 mM) in the experiments, it is assumed that [S] is negligibly different from the total surfactant concentration in the system.

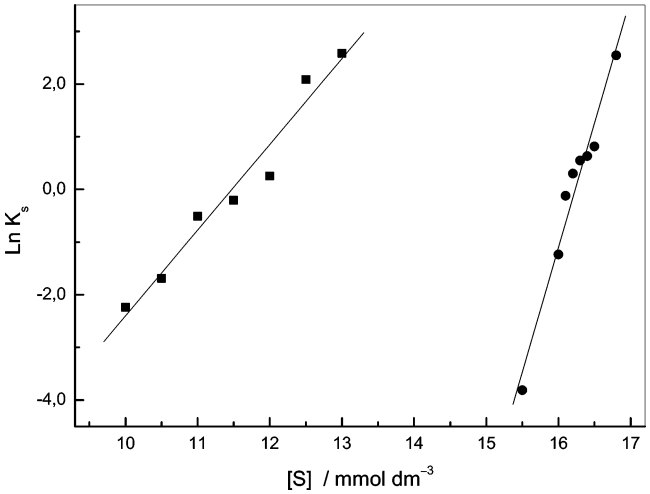

Figure 4. Relationship between K_S and ln[$C_7F_{15}COO^-$ Na^+] at 25 °C. (■) First transition (N → F_1). (●) Second transition (F_1 → F).

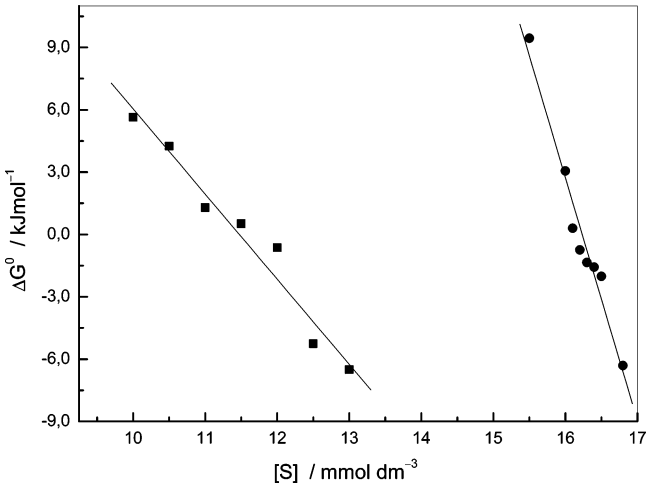

Figure 5. Standard Gibbs energy difference between two different protein conformations, 25 °C. (■) First transition (N → F_1). (●) Second transition (F_1 → F).

Values of K_S as a function of [S] for the first and second transition regions were calculated from the absorbance curve (A_{280}) in Figure 3, from the extent of denaturation (α) taken as

$$\alpha = \frac{A_{280} - A_{280}^{N}}{A_{280}^{D} - A_{280}^{N}} \tag{3}$$

where A_{280}^{N} and A_{280}^{D} are the absorbance for the native and denatured states, respectively, and $K_S = \alpha/(1 - \alpha)$. A_{280}^{N} and A_{280}^{D} were taken from the start and finish of the transition region. The pre- and posttransition curves were fitted by least-squares linear plots, and the transition region was fitted by a polynomial; α and K were then calculated by the method described by Pace.[24]

Figures 4 and 5 show plots of ln K_S and $\Delta G°$, respectively, as a function of surfactant concentration for the two transition regions. The linearity of $\Delta G°$ and ln K_S as a function of [S] is consistent with the following relations

$$\Delta G° = \Delta G_W^0 - m[S] \tag{4}$$

$$\ln K_S = \ln K_W - \frac{m}{RT}[S] \tag{5}$$

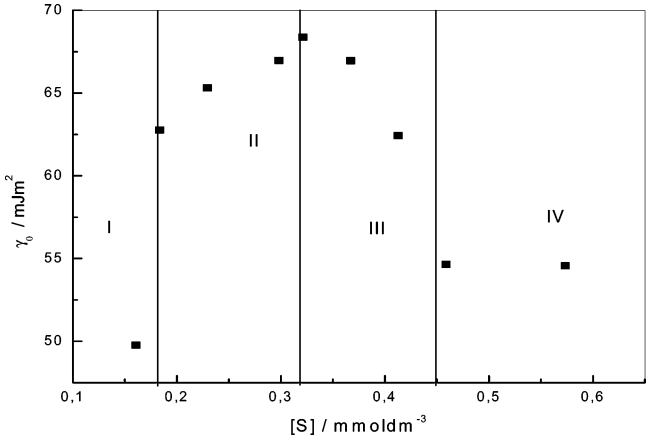

Figure 6. Equilibrium surface tension variation with [$C_7F_{15}COO^-Na^+$]. Estimated uncertainties are less than 2%.

SCHEME 1

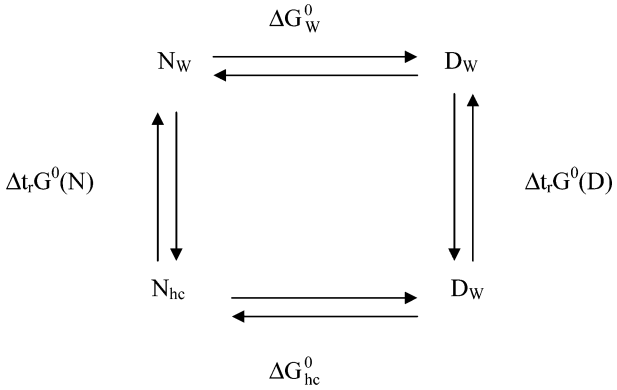

where $\Delta G°$ is the difference in the standard Gibbs energy between the folded and unfolded conformations. ΔG_W^0 is the value of $\Delta G°$ for the transition in the absence of surfactant, and m is a measure of the dependence of $\Delta G°$ on surfactant concentration.

Although there is some curvature in the plot of ln K_S vs [S], the curvature was not a consistent feature and analyses based on linearity were considered more appropriate than higher-order regression.

An equation of the form of eq 4 was found for protein denaturation by urea.[24,25]

From eq 2 it follows that

$$\ln K = \ln K_S - \nu \ln[S] \tag{6}$$

At a surfactant concentration of 1 mol dm^{-3}, ln K = ln K_S and the equilibrium constant might then be considered to correspond to the transition in a surfactant-saturated complex approximating that found in very hydrophobic environments with a corresponding Gibbs energy change, ΔG_{hc}^0. Least-squares analysis of the ln K_S vs ln[S] plots gave the value of ΔG_{hc}^0.

ΔG_{hc}^0 and ΔG_W^0 can be related by Scheme 1 from which follows that

$$\Delta G_{hc}^0 - \Delta G_W^0 = \Delta t_r G°(D) - \Delta t_r G°(N) \tag{7}$$

where $\Delta t_r G°$(D) and $\Delta t_r G°$(N) are the standard Gibbs energies of transfer of denatured and native HSA from water to a hydrophobic environments, respectively.

Table 1 lists the parameters $[S]_{1/2}$, m, ΔG_W^0, ν, ΔG_{hc}^0, and $\Delta(\Delta t_r G°)$ calculated from eqs 5, 6, and 7 for the HSA−$C_7F_{15}COO^-Na^+$ interactions.

TABLE 1: Parameters Characterizing the Surfactant-Induced Conformational Changes in Human Serum Albumin in Aqueous Solution at 25 °C

conformational transition	$[S]_{1/2}$/mmol dm^{-3}	m/kJ mol^{-1}	ΔG_W^0/kJ mol^{-1}	ν	ΔG_{hc}^0/kJ mol^{-1}	$\Delta(\Delta_t G°)$/kJ mol^{-1}
N → F_1	11.62 ± 0.19	4.1 ± 0.3	47.0 ± 4.1	18.5 ± 1.8	−205.5 ± 8.0	−252.5 ± 9.8
F_1 → F	16.18 ± 0.04	11.7 ± 0.9	190.0 ± 15.3	76.3 ± 5.9	−779.2 ± 25.1	−969.2 ± 38.2

Similar values for such parameters were obtained in previous works[26−29] and for the interactions between SDS and lysosyme.[30]

This suggests that the protein undergoes a conformational change due to the chemical interaction with $C_7F_{15}COO^-Na^+$, a briefly hydrophobic interaction, as shown by the ζ-potential data (Figure 2), and these conformational changes go through two steps. In the first step, the interaction is more electrostatic, as suggested by the ζ-potential data, and the surface protein charge increases as the surfactant concentration grows. However, in the second step the interaction is essentially hydrophobic; the ζ-potential values are constant. The narrow surfactant concentration, in the second step, and the higher values of the parameters that characterize the conformational change indicate that the interactions are cooperative.

Air−Aqueous Interface. The protein conformational changes in the bulk solution alter the HSA adsorption behavior at the air−aqueous interface. A general view of this fact can be estimated by analyzing the variation of equilibrium surface tension γ_0 ($t = \infty$) vs surfactant concentration.

Figure 6 shows the variation of equilibrium surface tension (γ_0, $t = \infty$) vs $[C_7F_{15}COO^-Na^+]$. The curve can be divided into four regions. In the first region, from $[C_7F_{15}COO^-Na^+] = 0.11$ mM to $[C_7F_{15}COO^-Na^+] = 0.18$ mM, (γ_0, $t = \infty$) increases with $[C_7F_{15}COO^-Na^+]$.

Increases in γ_0 at low concentrations of $C_7F_{15}COO^-Na^+$ are due to an interaction between surfactant and HSA molecules. Surfactant molecules act as a structure-stabilizing additive. Initially binding to sites with fairly high affinity leads to a strong increase in stability. This is shown in Figure 2, where the protein net charge increased. Previously,[11] we confirmed the surfactant-stabilizing capacity by UV−CD spectroscopy. A similar behavior was observed by SDS−BSA interaction.[5]

The compact structure of the protein excludes the water molecules from the interior. The absence of water facilitates the ionic interactions and the formation of hydrogen bonds among the residues. Inside the protein structure the hydrophobic residues are grouped whereas outside the polar groups are exposed.

$C_7F_{15}COO^-Na^+$ makes HSA molecules more hydrophilic, therefore, more water soluble and less surface active. The results are consistent with UV−vis spectroscopic measurements. Region I of Figure 6 coincides with the zone where the protein remains in its native state in the ABS vs $[C_7F_{15}COO^-Na^+]$ curve in Figure 3.

After an initial interaction, the increase in γ_0 is smoother. The same behavior is observed in the ζ-potential curve. This second region, from 0.18 to 0.34 mM, corresponds with the intermediate (F_1) formation. In this conformational form, the protein structure starts to open up and expose some of the hydrophobic residues, but not too many since this would cause a decrease in γ_0, just enough to produce a change in the slope of the plot.

In the third region, $[C_7F_{15}COO^-Na^+]$ from 0.34 to 0.46 mM, there is a decline in the (γ_0, $t = \infty$) values as $[C_7F_{15}COO^-Na^+]$ is augmented. This region corresponds in Figure 3 with the unfolded process.

When all of the basic sites on protein molecules are occupied by specifically bound surfactants, binding in this regimen is evidently due to favorable hydrophobic interactions between fluorocarbon tails of surfactants and possibly hydrophobic protein domains. These interactions lead to a conformational change of the protein structure. During this process, the hydrophobic residues on HSA molecules are being exposed, so proteins become more surface active and (γ_0, $t = \infty$) values decrease.

In the fourth region, $[C_7F_{15}COO^-Na^+]$ from 0.46 to 0.57 mM, (γ_0, $t = \infty$) remains constant and corresponds with a new protein conformation.

To evaluate extensively and intensively the way that conformational changes (induced by surfactant molecules) affect the adsorption of HSA at the air−aqueous interface, we studied the dynamic variation of surface tension (γ) and surface area (a) (Figures 7 and 8, respectively).

Figure 7 shows the surface tension variation with time; parts a, b, and c correspond to the low, middle, and high concentrations of $C_7F_{15}COO^-Na^+$ specifically.

At low $[C_7F_{15}COO^-Na^+]$, 0.160−0.183 mM, protein molecules are in their native state, as seen from absorbance measurements (Figure 3). At these surfactant concentrations, we obtain the typical $\gamma(t)$ curves for dilute protein solutions[31,32] (Figure 7a) that we have described for HSA−$C_7F_{15}COO^-Na^+$ interactions in a previous work.[11] So they absorb at the air−aqueous interface and manifest the typical three adsorption regimes of dilute protein solutions. The first is an induction regime, where the interfacial tension remains relatively constant at the pure fluid values. Regime II is characterized by a sharp decline in tension from this initial value, as the interface becomes saturated with protein. The final regime is a steady decline in interfacial tension, at a less negative slope than regime II on a semilog plot. It is attributed to conformational changes of the adsorbed layer and continued building of a gel-like network. The curves show an increase in the induction time with surfactant concentrations. When the $C_7F_{15}COO^-Na^+$ concentration increases, there are more surfactant molecules available to interact with HSA and therefore larger complexes are formed. In these complexes, protein structure is altered, as well as the rate flow. Therefore, regimes II and III change.

When we have a $C_7F_{15}COO^-Na^+$ concentration range of 0.23−0.39 mM (Figure 7b), spectroscopic UV−vis measurements show that protein molecules are in an intermediate configuration between the native and unfolded state, and the typical three regimes for dilute protein solutions disappear. The shape of the $\gamma(t)$ curves suggests that protein molecules, in this intermediate state, migrate from bulk to interface solution and form a monolayer. Surfactant concentration seems not to alter this behavior.

Finally, at high $[C_7F_{15}COO^-\ Na^+]$, Figure 7c, the adsorption of protein molecules exhibits a behavior analogous to that of dilute protein solutions. Protein molecules now present a new conformation in the bulk solution due to surfactant interactions. The protein molecules in this new conformational state are more hydrophobic than native protein molecules, so they move fast to the interface. Adsorbed molecules in the initial layer continue to change conformation in response to favorable environments for both hydrophobic and hydrophilic side chains. Later, overlap and entanglement of this layer occur, as the molecules seek more

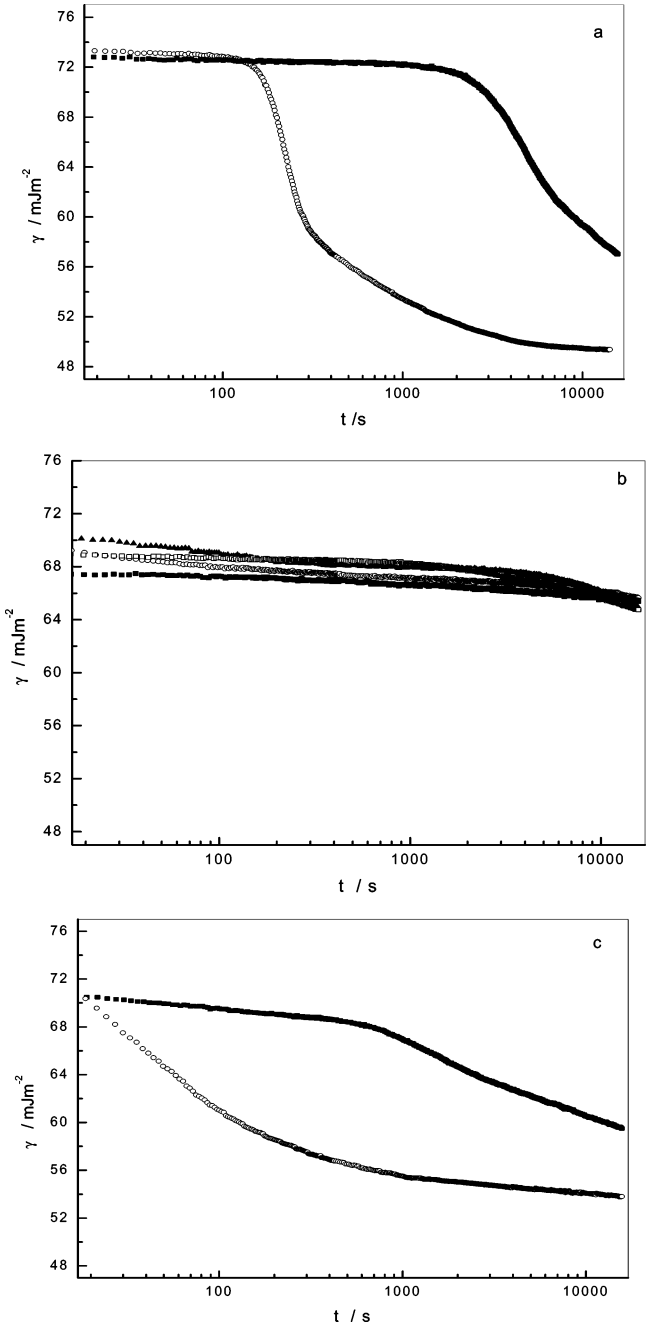

Figure 7. Dynamic surface tension measurements. HSA concentration was constant and equal to 0.45 μmol·dm^{-3}: (a) low surfactant concentrations, ○, 0.160 mmol·dm^{-3} $C_7F_{15}COO^-Na^+$, ■, 0.183 mmol·dm^{-3} $C_7F_{15}COO^-Na^+$; (b) middle surfactant concentrations, ■, 0.229 mmol·dm^{-3} $C_7F_{15}COO^-Na^+$, □, 0.298 mmol·dm^{-3} - $C_7F_{15}COO^-Na^+$, p, 0.321 mmol·dm^{-3} $C_7F_{15}COO^-Na^+$, ○, 0.367 mmol·dm^{-3} $C_7F_{15}COO^-Na^+$; (c) high surfactant concentrations, ■, 0.413 mmol·dm^{-3} $C_7F_{15}COO^-Na^+$, ○, 0.573 mmol·dm^{-3} - $C_7F_{15}COO^-Na^+$.

energetically favorable conformations. Multiple layers build into the water phase.

Often it is more convenient to express the data as a change in tension from the pure fluid value. This change is defined as the surface pressure

$$\pi(t) = \gamma_0 - \gamma(t)$$

where γ_0 is the interfacial tension of the pure fluids (in our case, water, $\gamma_0 = 72.8$ mJ/m^2).

To understand the form of the π vs t curves, it is necessary to know the dependence of π on Γ, as well as the variation of Γ with t. Γ can be related to the surface pressure, π, by the following equation

$$\pi(t) = RT[\Gamma(t)]^n \rightarrow \left(\frac{1}{\Gamma(t)}\right)^n = [a(t)]^n = \frac{RT}{\pi(t)}$$

where a is the surface area. When $n = 1$, the monolayer behaved like an ideal gas.

Figure 8 represents the surface areas (a) variation with t. The analysis of the curves was in complete accordance with the $\gamma(t)$ plots. The form of the curves implies that $n > 1$ for these systems.

At low surfactant concentration, the a vs t plots are divided into three regimes, the induction time, the monolayer saturation, and the interfacial gelation. The induction period is characterized by diffusion of proteins to the interface and initiation of conformational changes of adsorbed proteins molecules. There are few molecules at the interface, because so much surface area is available per molecule ($\approx$100 nm^2/molecule).

Strong adsorption arises from the presence of surface hydrophobic groups, and conformational changes occur. Unfolding of the proteins exposes new residues to the air phase, which also adsorb due to the similarities in environments of the nonpolar phase and interior of protein molecules. Surface areas change. Conformational changes of adsorbed HSA may provide a new environment for bulk protein molecules that approach the initial adsorbed layer.

There is a drastic decline in the a vs t curve (Figure 8a) that represents the variation of surface area during the conformational change. The interface becomes filled with protein molecules and HSA$-C_7F_{15}COO^-Na^+$ complexes which relax into less compact structures. The formation of multilayers may also be initiated.

Finally, there is a gradual fall in the surface area variation, which corresponds to initial gelation. In this regime, conformational changes of initial adsorbed layers continued. Multiple layers were built in the water phase, as the protein aggregated and formed branches. Aggregate branching forms an amorphous network compact structure.

At low concentrations, an increment in surfactant molecules in solution makes protein molecules more hydrophilic due to a structure-stabilizing effect. So HSA becomes less surface active and a_{eq} increases.

As the surfactant concentration increased, a_{eq} ($t = \infty$) augmented. When the surfactant concentration was 0.23$-$0.39 mM, the variation of surface area vs time was practically constant (Figure 8b). There was not an induction time or an interfacial gelation. Protein molecules migrate rapidly from the bulk to the interface and form a monolayer of about 0.8 nm^2/molecule. As with the surface tension values, surfactant concentration seems not to alter this behavior.

Finally, at high surfactant concentrations (Figure 8c), protein molecules are in their new conformational state. Due to their high hydrophobicity they move faster to the air$-$aqueous interface. The surface is saturated in a short period of time, so from the beginning there are small surface areas per molecule. Then, there is a gradual fall in the surface area variation. The adsorbed denatured HSA molecules may provide a new environment for bulk protein molecules that approach the initial adsorbed layer. Finally, a multilayer of denatured HSA molecules (about 0.2 nm^2/molecule) is formed.

Protein molecules, as a consequence of their interaction with the surfactant, change their native state (N) to a new and more

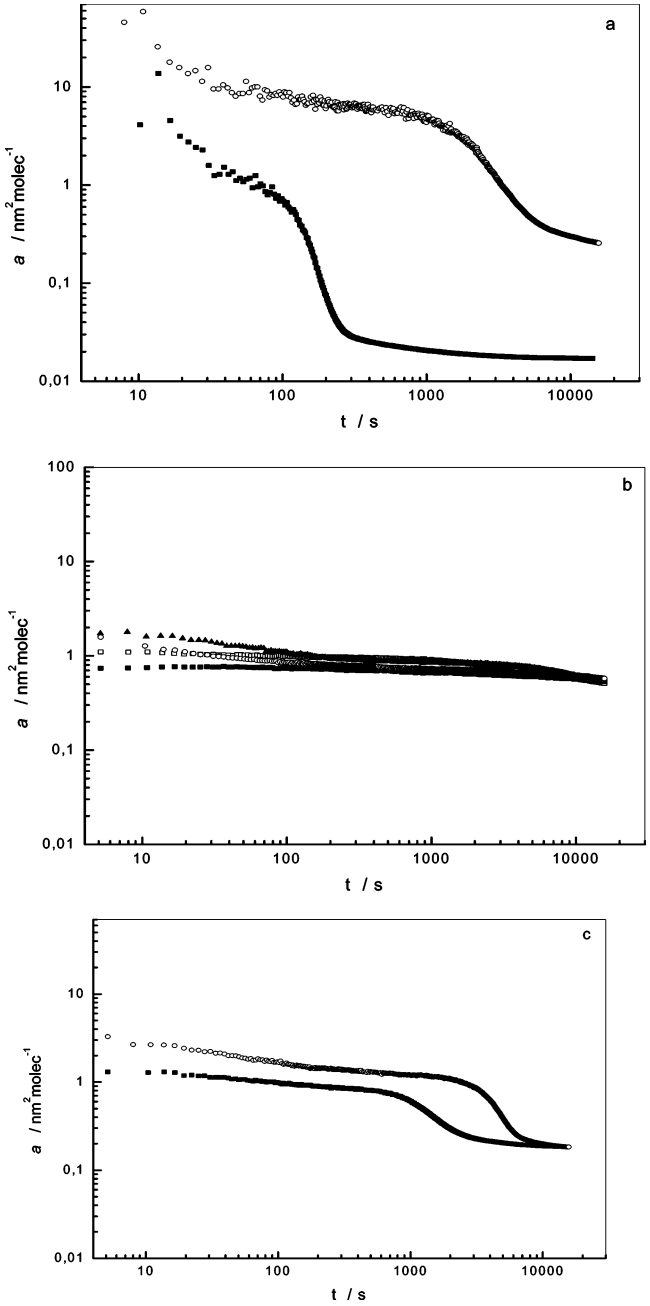

Figure 8. Dynamic surface area measurements. HSA concentration was constant and equal to 0.45 μmol·dm^{-3}: (a) low surfactant concentrations, ■, 0.160 mmol·dm^{-3} $C_7F_{15}COO^-Na^+$, ○, 0.183 mmol·dm^{-3} $C_7F_{15}COO^-Na^+$; (b) middle surfactant concentrations, ■, 0.229 mmol·dm^{-3} $C_7F_{15}COO^-Na^+$, □, 0.298 mmol·dm^{-3} - $C_7F_{15}COO^-Na^+$, ▲, 0.321 mmol·dm^{-3} $C_7F_{15}COO^-Na^+$, ○, 0.367 mmol·dm^{-3} $C_7F_{15}COO^-Na^+$; (c) high surfactant concentrations, ■, 0.413 mmol·dm^{-3} $C_7F_{15}COO^-Na^+$, ○, 0.573 mmol·dm^{-3} - $C_7F_{15}COO^-Na^+$.

hydrophobic conformational state (F). So much in its native state as in its new hydrophobic state, the protein tends to emigrate toward the air−aqueous interface and once there manifest the three typical regimes for diluted proteins. To change from its native form to the new conformational state, HSA molecules pass to an intermediate state. This can be seen in UV−vis measurements and ζ-potential data. Surface tension measurements and surface area data show that, in this intermediate state alone, few molecules reach the surface. As the protein consumes energy to change this intermediate conformational state, a lower tendency to occupy the surface exists.

Conclusion

Spectroscopic measurements indicated that HSA allows a transition between two conformational states. This transition is induced by the effect of surfactant $C_7F_{15}COO^-Na^+$ at a concentration below its critical micelle concentration and occurs in two steps.

The conformational transition of HSA by $C_7F_{15}COO^-Na^+$ was followed using absorbance measurements at 280 nm, and the data were analyzed to obtain the thermodynamic parameters of these conformational changes. Attending to the values of conformational change parameters, we found that the second transition is more hydrophobic and cooperative than the first.

Electrophoretical mobility (ζ-potential data) shows the formation of the HSA−$C_7F_{15}COO^-Na^+$ complex. The interactions are most likely hydrophobically driven, where both species carry the same charge sign.

These conformational changes in the bulk solution induce in each of the different conformational states of HSA molecules special adsorption behavior at the air−aqueous interface.

At low surfactant concentration, surfactant molecules act as a structure-stabilizing additive. Initially, binding to sites with fairly high affinity leads to an increase in stability. So HSA molecules absorb at the air−aqueous interface and manifest the typical three adsorption regimes of dilute protein solutions. When all the sites on the protein molecules are occupied by specifically bound surfactants and surfactant concentrations increase, the binding is due to favorable hydrophobic interactions between fluorocarbon tails of surfactants and possibly with hydrophobic protein domains. These interactions lead to a conformational change in protein molecules. The shape of the $\gamma(t)$ curves suggests that protein molecules pass to an intermediate state between two conformational forms. In this intermediate state, they migrate from bulk to interface solution and form a single layer. Surfactant concentration seems not to alter this behavior.

At high surfactant concentration, $\gamma(t = \infty)$ remains constant and corresponds with the total change of protein conformation. Protein molecules at this new conformational state are more hydrophobic than native proteins. So they move quickly to the interface. Adsorbed molecules in the initial layer continue to change conformation in response to favorable environments for both hydrophobic and hydrophilic side chains. Later, overlap and entanglement of these layers occur, as the molecules seek more energetically favorable conformations. Multiple layers are built in the water phase.

Acknowledgment. This research was funded by the Spanish Ministry of Science and Technology (Project MAT2002-00608, European FEDER support included) and by Xunta de Galicia (Project PGIDIT03PXI20615PN). P. V. Messina thanks Fundación Antorchas, Argentina (14308/110), and Banco Rio, Argentina.

References and Notes

(1) Peters, T., Jr. *All about Albumin: Biochemistry, Genetics, and Medical Applications*; Academic Press Inc.: San Diego, CA, 1996.

(2) Carter, D. C.; Ho, J. X. *Adv. Protein Chem.* **1994**, *45*, 153.

(3) Figge, J.; Rossing, T. H.; Fencl, V. *J. Lab. Clin. Med.* **1991**, *117*, 456.

(4) Herve, H.; Urien, S.; Albengres, E.; Duche, J. C.; Tillement, J. *Clin. Pharmacokinet.* **1994**, *26*, 44.

(5) Deep, S.; Ahluwalia, J. C. *Phys. Chem. Chem. Phys.* **2001**, *3*, 4583.

(6) Gelamo, E. L.; Silva, C. H. T. P.; Imasato, H.; Tabak, M. *Biochim. Biophys. Acta* **2002**, *1594*, 84.

(7) Sesta, B.; Gente, G.; Iovino, A.; Laureti, F.; Michiotti, P.; Paiusco, O.; Palacios, A. C.; Persi, L.; Princi, A.; Sallustio, S.; Sarnthein-Graf, C.; Capalbi, A.; La Mesa, C. *J. Phys. Chem. B* **2004**, *108*, 3036.
(8) Han, Xing; Snow, T. A.; Kemper, R. A.; Jepson, G. W. *Chem. Res. Toxicol.* **2003**, *16*, 775.
(9) Fukushima, K.; Sugihara, G.; Murata, Y.; Tanaka, M. *Bull. Chem. Soc. Jpn.* **1982**, *55*, 3113.
(10) Prieto, G.; Sabín, J.; Ruso, J. M.; González-Pérez, A.; Sarmiento, F. *Colloids Surf., A* **2004**, *249*, 51.
(11) Messina, P. V.; Prieto, G.; Ruso, J. M.; Sarmiento, F. *Langmuir*. Submitted for publication.
(12) Dockal, M.; Carter, D. C.; Rüker, F. *J. Biol. Chem.* **2000**, *275*, 3042.
(13) Hunter, J. R. *Zeta Potential in Colloid Science*; Academic Press: London, 1981.
(14) Foster, J. F. In *Albumin Structure, Function and Uses*; Rosenoer, V. M., Oratz, M., Rothschild, M. A., Eds.; Pergamon: Oxford, U.K., 1977.
(15) Geisow, M. J.; Beaven, G. H. *Biochem. J*. **1977**, *163*, 477.
(16) Khan, M. Y. *Biochem. J*. **1986**, *236*, 307.
(17) Foster, J. F. In *The Plasma Proteins*; Putnam, F. W., Ed.; Academic Press: New York, 1960; Vol. 1.
(18) Harrington, W. F.; Johnson, P.; Ottewill, R H. *Biochem. J.* **1956**, *62*, 569.
(19) Sogami, M.; Era, S.; Nagaoka, S.; Inouye, H. *Int. J. Pept. Protein Res.* **1982**, *19*, 263.
(20) Era, S.; Kuwata, K.; Kida, K.; Sogami, M.; Yoshida, A. *Int. J. Pept. Protein Res.* **1985**, *26*, 575.
(21) Taylor, R. P.; Chau, V.; Zenkowich, M. J.; Lake, L. H. *Biophys. Chem.* **1978**, *7*, 293.
(22) Kaufmann, W.; Simpson, R. B. *J. Am. Chem. Soc.* **1953**, *75*, 5154.
(23) Rudolph, R.; Holler, E.; Jaenicke, R. *Biophys. Chem.* **1975**, *3*, 226.
(24) Pace, C. N. *Tibtech.* **1990**, *8*, 93.
(25) Pace, C. N.; Laurents, D. V. *Biochemistry* **1989**, *28*, 2520.
(26) Housaindokht, M. R.; Jones, M. N.; Newall, J. F.; Prieto, G.; Sarmiento, F. *J. Chem. Soc., Faraday Trans.* **1993**, *89*, 1963.
(27) Prieto, G.; Suárez, M. J.; González-Pérez, A.; Ruso, J. M.; Sarmiento, F. *Phys Chem. Chem. Phys.* **2004**, *6*, 816.
(28) Pombo, C.; Suárez, M. J.; Nogueira, M.; Czarnecki, J.; Ruso, J. M.; Sarmiento, F.; Prieto, G. *Eur. Biophys. J.* **2001**, *30*, 242.
(29) Jones, M. N.; Prieto, G.; Del Rio, J. M.; Sarmiento, F. *J. Chem. Soc., Faraday Trans.* **1995**, *91*, 2805.
(30) Sun, M. L.; Tilton, R. D. *Colloids Surf. B* **2001**, *20*, 281.
(31) Beverung, C. J.; Rodke, C. J.; Blanch, H. W. *Biophys. Chem.* **1999**, *81*, 59.
(32) Wege, H. A.; Holgado-Terriza, J. A.; Cabrerizo-Vilchez, M. A. *Prog. Colloid Polym. Sci.* **2004**, *123*, 188.